Catalysis Science & Technology

Accepted Manuscript

ROYAL SOCIETY OF CHEMISTRY

www.rsc.org/catalysis

Journal Name

RSCPublishing

ARTICLE

Enhanced Catalytic Activity of Au Nanoparticles Self-Assembled on Thiophenol Functionalized Graphene

Ren Ren, Shuwen Li, Jing Li, Jianxin Ma, Hengzhi Liu and Jiantai Ma.*

Cite this: DOI: 10.1039/x0xx00000x

Received ooth January 2012,
Accepted ooth January 2012

DOI: 10.1039/x0xx00000x

www.rsc.org/

A new catalyst containing 1-2 nm Au nanoparticles) anchored to thiophenol covalently functionalized graphene sheets (Au/TP-GS) was fabricated using a facile, synthetic approach. The details of the morphologies, size and dispersion of the Au nanoparticles (NPs) and the chemical composition of the novel catalyst was verified by systematic characterizations, including transmission electron microscopy (TEM), high-resolution transmission electron microscopy (HRTEM), Raman spectroscopy, X-ray diffraction (XRD) and X-Ray photoelectron spectroscopy (XPS). The resulting Au/TP-GS exhibited excellent catalytic activity for both the reduction of 4-nitrophenol and the photodegradation of rhodamine B due to the synergistic effects between the TP-GS and Au NPs and the high utilization of the metal. The practical and efficient nanocatalyst synthesized by a facile in-situ reduction approach, provides more environmentally benign synthesis route to effectively produce low cost Au-based catalysts.

Introduction

Noble metal NPs have received enormous interest in a wide variety of applications, especially in heterogeneous catalysis owing to their large specific surface areas and large number of exposed metal atoms, which greatly enhances their catalytic and physicochemical properties.[1, 2] Gold (Au) nanoparticles have attracted considerable attention due to their unique physical and chemical properties and their very important applications in catalysis. Typical reaction examples include, the reduction of 4-nitrophenol (4-NP) to 4-aminophenol (4-AP),[3, 4] low-temperature carbon monoxide oxidation, propylene epoxidation,[5, 6] the oxidation of alcohols,[7, 8] the photocatalytic degradation of dyes,[9, 10] the electrochemical CO_2 reduction[11] and formic acid dehydrogenation.[12] In particular, the reduction of 4-NP on Au nanocatalysts in the presence of $NaBH_4$ has been intensively investigated for efficient production of 4-AP, which is well known as an important intermediate for the manufacture of analgesic and antipyretic drugs.[13] 4-aminophenol is also widely used as a photographic developer, corrosion inhibitor, anticorrosion-lubricant and hair-dyeing agent.[14]

Large quantities of dyes are produced annually and used in a variety of industries including textile, cosmetic, paper, leather, pharmaceutical and nutrition industries. The presence of even trace concentrations of dyes in the effluents from these industries is highly visible and undesirable. Dye pollutants can have serious detrimental effects on aquatic life and human health. With the increase in international environmental awareness, new, cost effective green routes for treating dye-containing wastewater are being sought. These environmental concerns have led to new, stricter regulations concerning colored wastewater discharge as well as the development of more efficient treatment technologies[15, 16] to remove these offending substances. Of the available catalysts for use in degrading recalcitrant substances such as dyes in wastewater, Au NPs is recognized as an extraordinary example.[17] However, Au nanoparticles are known to easily aggregate due to their high surface energy, resulting in a marked reduction in their original catalytic activity. Hence, Au nanoparticles are generally anchored on a variety of supports including polymers,[4, 18] metal oxides,[19-21] carbon materials,[22, 23] to help prevent this agglomeration. To increase the active surface area of these composite catalysts, one promising strategy is to decrease the size of particles or form noble-metal shells using inexpensive metal or alloy in the core region of the catalyst. However, decreasing the particle size to several nanometers is limited by the conventional synthesis methods that utilize surfactants or dendrimers as templates, which; unfortunately, can form barriers that confining the catalytic activity. Consequently, it is necessary to develop a surface containing a

plethora of evenly dispersed nanoparticles to maintain the level of catalytic activity.

To this end, graphene is under consideration as a new support. Graphene is a novel 2D material that is a single layer of closely stacked carbon atoms are in a two-dimensional honeycomb lattice.[24] Graphene has high specific surface area (calculated value 2639 $m^2 g^{-1}$), high conductivity (103–104 S m^{-1}) and a

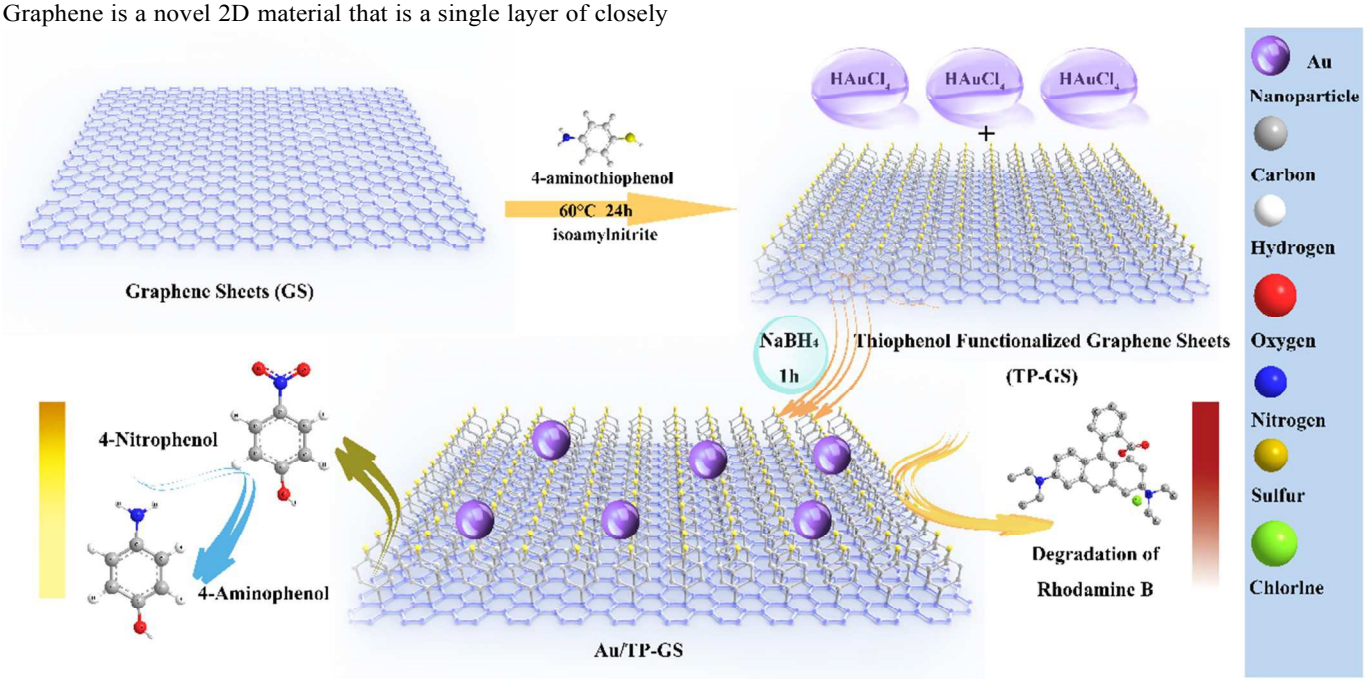

Scheme 1 Illustration of the formation of TP-GS and Au/TP-GS, as applied to the reduction of 4-nitrophenol and photodegradation of rhodamine B.

relatively low cost.[25] Because of its unique structure and the prominent properties, graphene has potential applications in the fabrication of nanocomposites and various microelectronic devices. Graphene-nanoparticle composites are usually synthesized by an in situ reduction of a functionalized graphene/metal salt complex, as has been reported earlier by our group.[26-28] Due to the large bond energy of the Au-SH coordination bonds, carbon nanotubes can be successfully functionalized using 4-aminothiophenol (4-ATP).[29] Thus, in this study, the plan was to prepare thiophenol functionalized graphene sheets containing covalently bonded 4-ATP. The resulting material functionalized by covalent bonding can then be homogeneous distributed in solution and would be much stronger than a similar material functionalized via non-covalent π–π stacking.

In this study, a new catalyst (Au/TP-GS), was fabricated using Au NPs (only 1-2 nm) which were anchored to the thiophenol functionalized graphene sheets via covalent bonds, using a facile, one-pot synthetic approach (Scheme 1). Systematic characterization, including transmission electron microscopy (TEM), high-resolution transmission electron microscopy (HRTEM), Raman spectroscopy, X-ray diffraction (XRD) and X-Ray photoelectron spectroscopy (XPS) was conducted to define the morphologies, dispersion of Au nanoparticles (NPs) and the chemical composition of the novel catalysts. The activities of the catalyst for the reduction of 4-NP to 4-AP and the degradation of rhodamine-B were determined. These activities were found to be excellent, possibly as a result of the high utilization of the gold, the unique connection between each part of the catalyst and the good adsorption capacity between graphene sheets and the aromatic compounds.

Experimental Section

Materials

Graphene sheets (GS, 95%) were purchased from Nanjing XFNano Materials Tech Co., Ltd, China. $HAuCl_4$ (99%), sodium borohydride ($NaBH_4$) was purchased from Aldrich. 1,2-dichlorobenzene (ODCB), 4-aminothiophenol (4-ATP), isoamylnitrite, 4-nitrophenol and (4-NP) rhodamine B (RhB) were purchased from Alfa Aesar. All other reagents were purchased from the Tianjin Guangfu Chemical Co. Ltd. Water used in the experiments was deionized and doubly distilled.

Synthesis of Thiophenol Fuctionalized Graphene Sheets (TP-GS)

15mg of graphene sheet (GS) were devoted in 20ml ODCB using ultrasonication for 30min. The suspension was added to a solution of the 0.72g 4-aminothiophenol in 10ml acetonitrile, then purged with Ar for 15min. Following this, 1.71ml of isoamylnitrite was quickly to the solution added via syringe. The mixed suspension was vigorous stirred at 60°C for 24h under an inert atmosphere. After cooling to room temperature, the suspension was diluted with dimethylformamide (DMF), filtered through a PTFE membrane disc filter (0.45 μm pore size) under vacuum followed by extensive washing with DMF until the filtrate became colorless to ensure removal of excess,

untreated 4-aminothiophenol and isoamylnitrite. DMF was removed by washing with a sufficient quantity of absolute ethanol. The thiophenol-functionalized GS was obtained which is heretofore denoted as TP-GS.

Preparation of Au/TP-GS Composite Materials.

The TP-GS was ultrasonically suspended in 20ml DI water containing 3.5ml ethanol for 30min, then purged with Ar for 25min. A solution of $HAuCl_4$ (0.1 ml 20mM diluted to 20ml) was then added dropwise with stirring. After 10min of mixing, a freshly prepared solution of $NaBH_4$ (15mg in 30ml of H_2O) was added dropwise to the mixture. After 45min of reaction, the product was collected by filtering through a PTFE membrane disc filter (0.45μm pore size) under vacuum, then washed several times with H_2O and ethanol. The final product was dried in a vaccum oven at 40°C overnight.
The Au/GS was also prepared in the same procedure except that the TP-GS was replaced by the GS.

Characterization

Transmission electron microscopy (TEM) and high resolution TEM (HRTEM) images were obtained using a FEI-TECNAI G^2 transmission electron microscope operating at 200 kV (FEI company). Elemental composition data of the product was collected using energy dispersive X-ray spectroscopy (EDS) performed on a TECNAI G^2 microscope. Raman spectra were recorded using a Via Reinishaw confocal spectroscope with 633 nm laser excitation. XRD measurements were conducted at room temperature and performed using a Rigaku D/max-2400 diffractometer employing Cu-Kα radiation as the X-ray source in the 2θ range of 10–90°. X-ray photoelectron spectroscopy (XPS) analysis was conducted using a PHI-5702 X-ray photoelectron spectrometer. UV–Vis absorption spectra were recorded using a T6 UV–Vis spectrophotometer. Inductive coupled plasma atomic emission spectroscopy (ICP-AES) analysis was conducted using a PerkinElmer (Optima-4300DV).

Catalytic Reduction of 4-Nitrophenol

A sample of fresh $NaBH_4$ solution (1.5 mL, 2.5 mM) was added to a 4-NP solution (1.47 mL, 0.025 mM) in a quartz cuvette. Subsequently, the as-prepared Au/TP-GS (20 μL, 1 mg mL^{-1}) was added. Immediately after adding the catalyst, UV–Vis spectrum of the sample was recorded at 30 second intervals at 25°C. To study the reusability of the as-prepared catalyst, the reduction reaction was amplified 20 times. The Au/TP-GS were separated by brief centrifugation, washed with water, and dried in vacuo at temperature for the next cycle of catalysis. This procedure was repeated five times.

Photocatalytic Reaction of Rhodamine B

Photocatalytic measurements were conducted in an open thermostatic photoreactor. Before irradiation, a suspension containing 100 mL of 0.9×10^{-2} mM Rhodamine B (RhB) solution and 5 mg of the solid Au/TP-GS catalyst was sonicated for 5 min and stirred for 60 min in the dark to allow for sorption equilibrium. Then, the mixture was irradiated with a 500 W halogen lamp equipped with a 420nm cut-off filter. At select time intervals of irradiation, corresponding 5 mL aliquots of the test solution were withdrawn. The residual concentration of RhB in the aliquots was analyzed using a UV-Vis spectrophotometer.
The Au/TP-GS composites, previously used in the degradation experiment were tested for its ability to be reused multiple times. The catalyst were gained by filtration and cleaned by immersing them in ethanol for 6 hours. Then they were rinsed five times with deionized water, and dried at 80°C in hot air oven. After the Au/TP-GS were cleaned, they were reused for the removal of dyes by repetition of the experiments. This procedure was repeated five times.

Results and Discussion

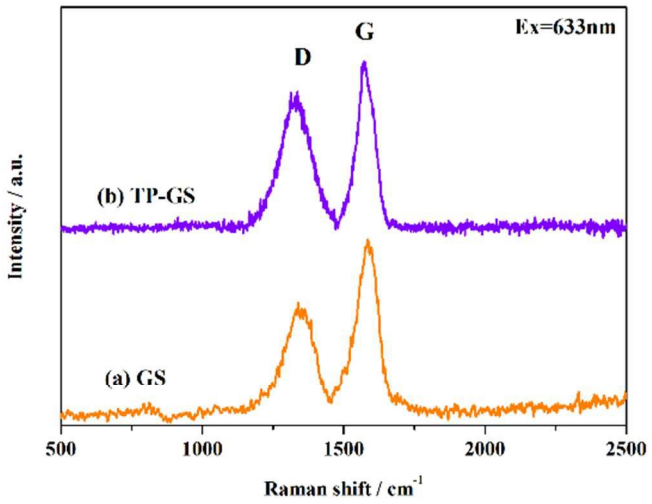

Fig. 1 Raman spectra of (a) GS and (b) TP-GS

Fig. 1 shows the Raman spectra of the GS and the TP-GS with 633 nm laser excitation. As expected, two characteristic peaks (D band, 1311 cm^{-1} and G band, 1587 cm^{-1}) were clearly observed for the GS and the TP-GS. The D band can be assigned to the A_{1g} breathing mode of the disordered graphite structure, due to the defect sites in the hexagonal framework of graphite materials. The G band can be assigned to the E_{2g} structure mode of graphite,[30, 31] which reflects the structure of the sp^2 hybridized carbon atoms. The level of chemical modification of the graphitic carbon sample is commonly quantified by the intensity ratio of the D band and G bands (I_D/I_G).[31, 32] Therefore, it was noteworthy that the I_D/I_G ratio of the TP-GS (0.843) was larger than that of the pristine GS (0.594). This tendency is due to an increase in the number of sp^3 carbons which were formed on the graphene as a result of the chemical functionalization. This result indicates that the functionalization of GS by the 4-aminothiophenol molecules via covalent bonds was successful.[33] The results of Raman spectroscopy confirmed that the functionalization was efficient

and the TP-GS should be a promising catalyst support for noble metals.

Fig. S1 shows FTIR spectrum of (a) 4-aminothiophenol, (b) GS and (c) the GS functionalized with mercaptobenzene moieties. By comparing with infrared spectra of curves (a) and (b), the peaks centered at 1620 and 1578cm^{-1} are due to C-C stretching vibration of the benzene rings that attached to GS. The peaks centered at 1460 and 1488cm^{-1} are related to the mixed C-C stretching and C-H bending vibration of benzene rings. The peak centered at 816 cm^{-1} is a well-known C-H out-of-plane bending vibration in paradisubstituted benzene. All mentioned peaks could be attributed to the presence of mercatophene moieties attached to the GS.

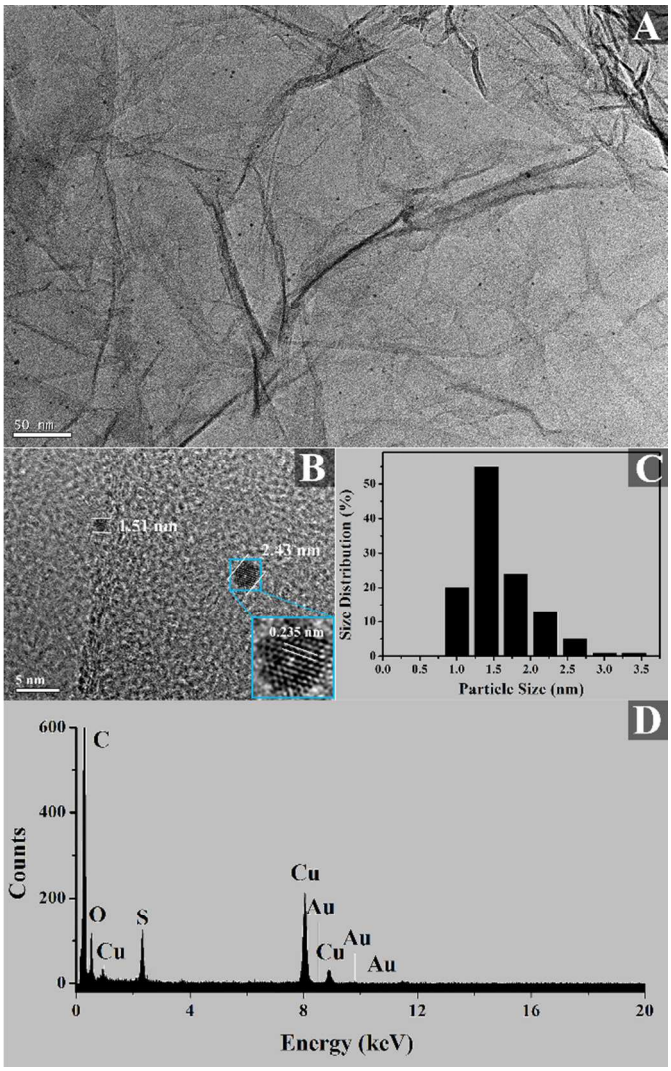

Fig. 2 Typical TEM (A) and HRTEM (B) images of Au/TP-GS, size distribution histograms (C) of image (A) and EDS Spectrum of Au/TP-GS

TEM was used to investigate the morphology and structure of the Au/TP-GS (Fig. 2) and Au/GS (Fig. S1). According to Fig. 2A, the narrow size distribution of the quasi-spherical shaped Au NPs were equally covered on the surface of TP-GS. The average diameter of the particles was about 1.5 nm (Fig. 2C), while which was about 8-12 nm in Au/GS. High-resolution TEM (HRTEM) analysis of the materials revealed the highly crystalline nature of the Au NPs with a lattice spacing of 0.235 nm which was indicative of the lattice spacing of the (111) planes of Au.[34] The elements in the nanocomposite were identified by energy dispersive X-ray spectroscopy (EDS) which is shown in Fig. 2D. According to EDS, C, S and Cu are the predominant species, while Au is inconspicuous, because of its very low content (<1%, identified by ICP-AES) in the catalyst.

It is obvious that the existence of mercaptobenzene influence the morphology of metal/graphene composites. Owing to the large bond energy of the Au-SH coordination bonds, the Au nanoparticles anchored on the functionalized carbon layer with a very small size, a narrow and homogeneous distribution. On the contrary, Au NPs were randomly dispersed on non-functionalized GS and some of them appeared aggregation with a wide size distribution (Fig. S2).

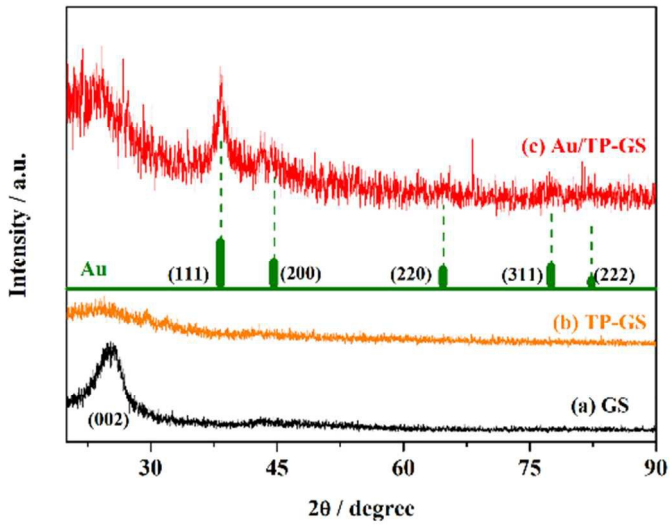

Fig. 3 XRD patterns of (a) GS, (b) TP-GS and (c) Au/TP-GS. For comparison, the XRD pattern of Au from the Joint Committee Powder Diffraction Standard (JCPDS) are also presented.

Fig. 3 displays the XRD patterns of the GS and TP-GS composites. In this figure, the pattern of GS is represented by the (a) line and the pattern of TP-GS is represented by the (b) line. The diffraction peak centered at around 25° can be attributed to the (002) plane. The broadening of the diffraction peak (002) indicated the formation of the graphene nanosheets.[35] The intensity of TP-GS peaks was smaller than the GS peaks, indicating that the process of functionalization changed the structure of GS, which confirms that the functionalization *via* covalent bonds is highly efficient. The (c) shows the XRD patterns of the Au/TP-GS. Compared with the Joint Committee Powder Diffraction Standard (JCPDS) for pure Au (No. 89-3697), the diffraction pattern of Au NPs can be assigned to the (111), (200), (220), (311) and (222) planes of a face centred cubic (fcc) lattice.

To further characterize the surface chemical composition of the prepared catalysts, XPS analysis of TP-GS and Au/TP-GS was

performed. Fig. 4 shows typical survey XPS spectra of the TP-GS and Au/TP-GS (Fig. 4A) and the high resolution XPS spectra for Au and S in Au/TP-GS and S in TP-GS (Fig. 4B, C and D, respectively). Fig. 4B shows Au $4f_{7/2}$ and $4f_{5/2}$ doublet with binding energies of 83.78 eV and 87.43 eV, respectively. The Sp2 photoelectron peaks shown in Fig. 4C and Fig. 4D correspond to the S element in Au/TP-GS and TP-GS, respectively. The Sp2 peak of TP-GS appeared at 164.21eV, compared to 163eV for thiophenol. The small shift to a higher energy indicated that the thiophenol was bonded to an electron withdrawing group on the graphene. The energy of Sp2 peak of Au/TP-GS, showed a slight shift of about 0.4 eV in the gold-containing samples, with respect to the corresponding pure support alone,[36] which may be attributed to a charge compensation effect.[37]

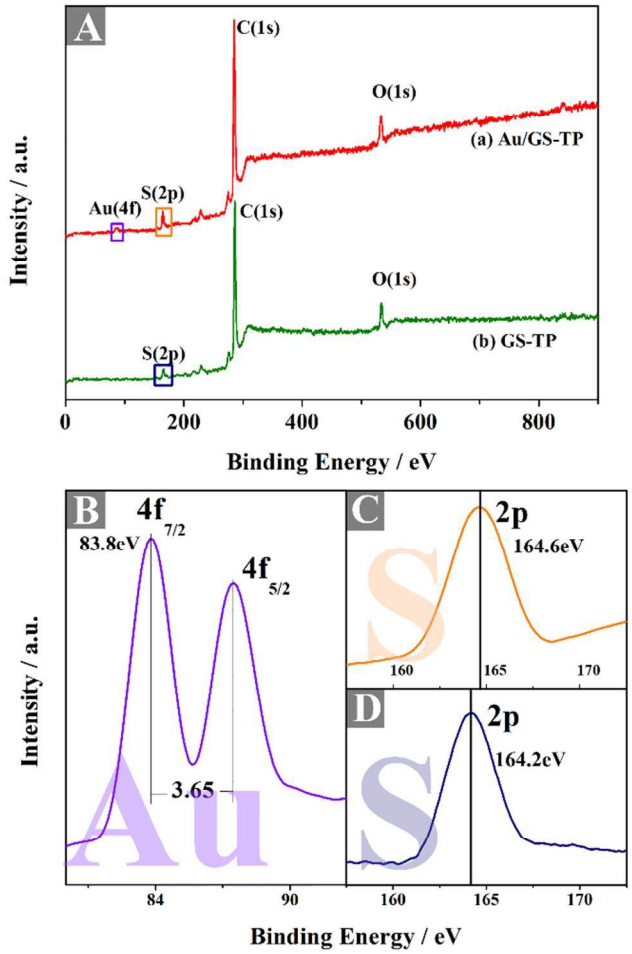

Fig. 4 XPS Wide-Scan (A-a) and Au 4f (B), S 2p (C) High-Resolution Spectra of the Au/TP-GS, Wide-Scan(A-b) and S 2p (D) High-Resolution Spectra of TP-GS.

The catalytic reduction of 4-NP on noble metal NPs has often been used as one of the model reactions to evaluate the catalytic performance of various metal NPs.[38, 39] Additionally, the successful conversion reaction can be monitored by measuring the change in the light absorbance of the reaction mixture, because the reaction proceeds readily and only one product is formed. Initially, the 4-NP solution was light yellow in colour, which then turned dark yellow upon the addition of $NaBH_4$ due to the formation of 4-nitrophenolate.[40] Then, the UV–Vis absorption spectrum of the aqueous mixture of 4-NP and $NaBH_4$ had an absorption maximum at 400 nm corresponding to the presence of 4-nitrophenolate. With addition of the catalyst, the absorption intensity of 4-NP at 400 nm decreased with the time and a new peak developed at 310 nm which was attributing to 4-AP (Fig. 5A). As the reaction proceeded, it was obvious that the concentration of the reactant (4-NP) decreased linearly, but the

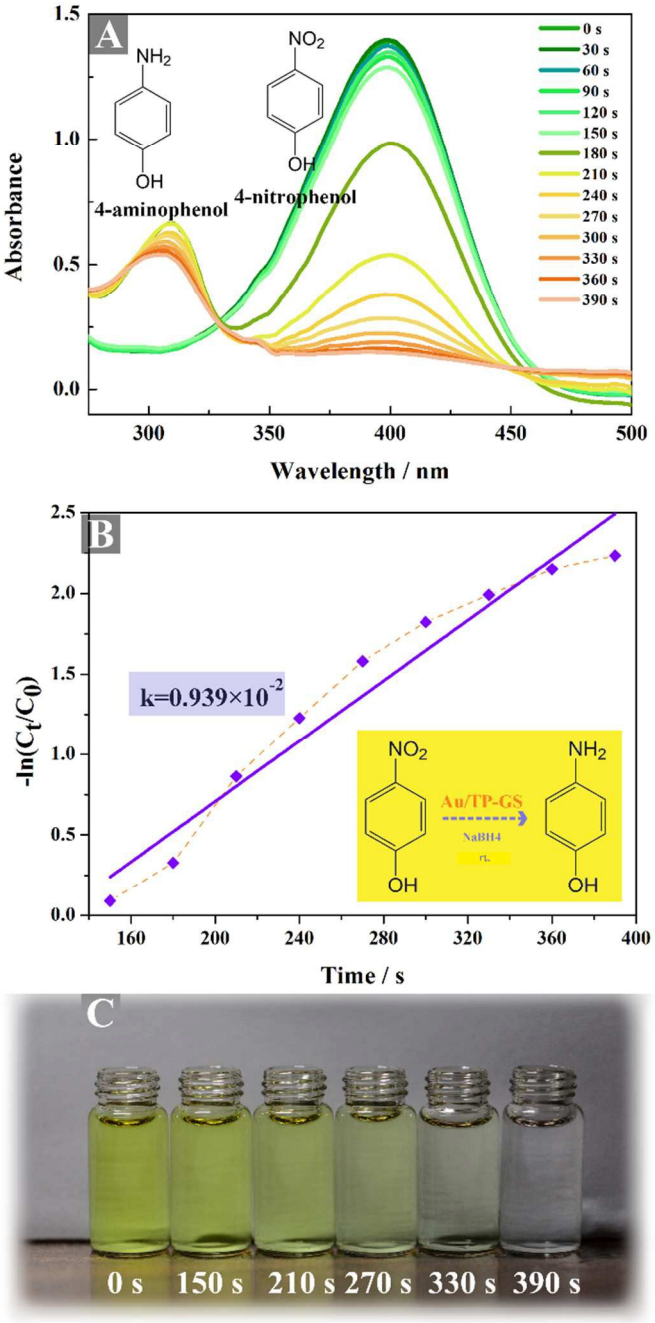

Fig. 5 (A) Representative time dependent UV–Vis absorption spectra for the reduction of 4-NP on Au/TP-GS in water at 25°C. (B) Plot of –ln (C_t/C_0) versus time spectra for the reduction of 4-NP on Au/TP-GS. (C) The temporal evolution color change for the 4-NP reduction using the Au/TP-GS catalyst.

concentration of the product did not. This was attributed to the absorption of some of the 4-AP by the graphene sheets as a result of the π-π absorption. Fig. 5B shows the plot of –ln (C_t/C_0) (C_t = concentration at time t, C_0 = concentration at t = 0) as a function of time (in seconds), which allows for the determination of the rate constant (k). As previous studies have shown, there is an induction time, which corresponds (assuming a Langmuir–Hinshelwood mechanism) to "an activation or restructuration of the metal surface by the nitrophenol"[41, 42] prior to the actual reduction reaction. Then, the reaction follows a pseudo-first order rate as is usually accepted.[43, 44] Fig. 5C shows the change in colour of the reaction system with time. The rate constant k was calculated to be 0.939×10^{-2} S^{-1}.

In order to compare the results with reports in the literature, the ratio of the rate constant k with respect to the total weight of the catalyst was calculated (k_o= k/m) under similar reaction conditions. Then, the activity factor k_o of the Au/TP-GS was found to be 539 $s^{-1}g^{-1}$, which was much larger than that of Au/GS (k_o= 232 $s^{-1}g^{-1}$, shown in Fig. S4) and some other Au/GS composites in related reports.[45] The improved result indicated that the Au/TP-GS possessed a high catalytic activity for this reaction under similar reaction conditions.

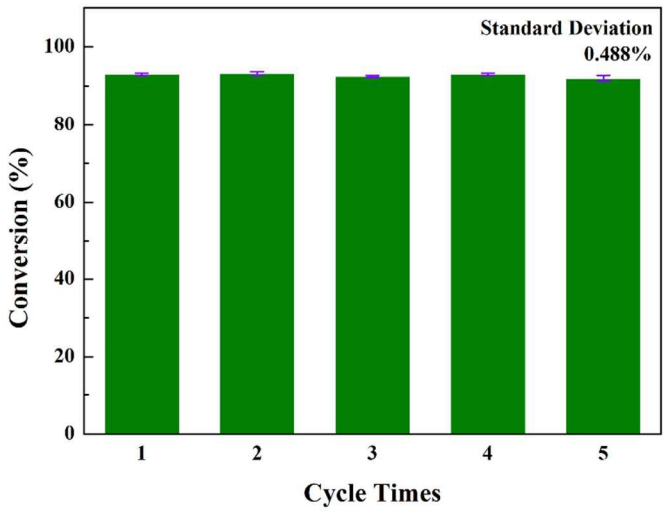

Fig. 6 The reusability of Au/TP-GS as a catalyst for the reduction of 4-NP with $NaBH_4$.

The Au/TP-GS catalyst could be recovered from the reaction mixture by brief centrifugation or filtration. As shown in Fig.6, the recovered Au/TP-GS catalysts exhibited nearly the same catalytic activity as the "virgin" catalyst for at least five successive cycles of the reduction reaction with a stable conversion of 93% within 400 s. This result clearly indicated that Au/TP-GS catalysts possessed good stability.

The photoactivity of Au/TP-GS was evaluated using rhodamine B (RhB) under visible light irradiation. The target substrate RhB, which contains four N-ethyl groups at either side of a xanthene ring is relatively stable in aqueous solutions subjected to visible light irradiation.[46] Furthermore, it is known that a reaction has not observed in this system in the presence of either TiO_2 (in this paper, we used P25 as a comparison) or Au NPs. However, RhB underwent pronounced photodegradation in the presence of either of the two subject catalysts upon irradiation with visible light. The UV-visible spectral changes during the photodegradation of RhB in the presence of Au/TP-GS and the absorption intensity of RhB gradually decreased with increasing irradiation time without any shift of the absorption wavelength

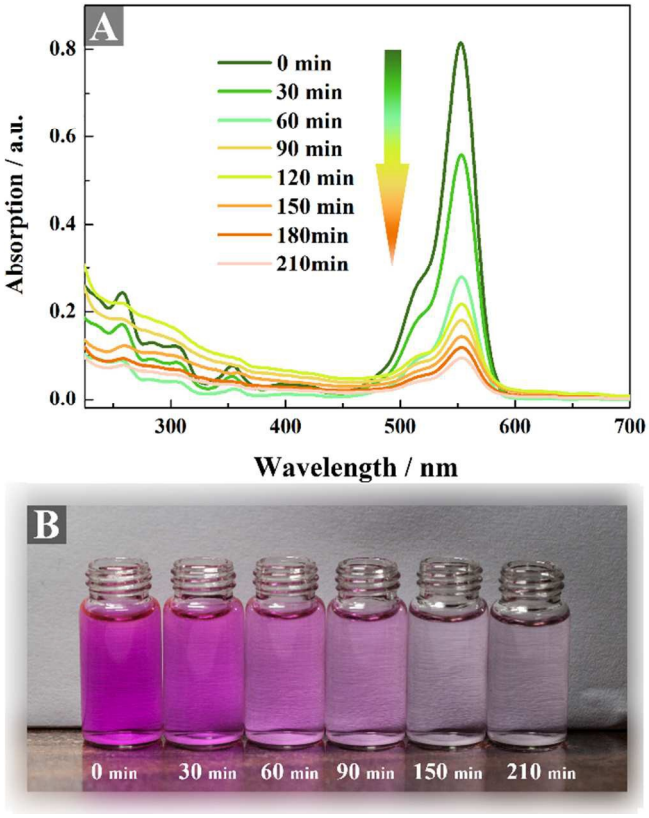

Fig. 7 (A) Absorption profiles of RhB vs irradiation time in the presence of Au/TP-GS. (B) The temporal evolution of colour change of RhB photodegradation using the Au/TP-GS Catalyst.

(Fig. 7A). This suggested a complete cleavage of RhB chromophores.[10] Fig. 7B shows that the colour of the reaction changes with time during the degradation catalysed by Au/TP-GS.

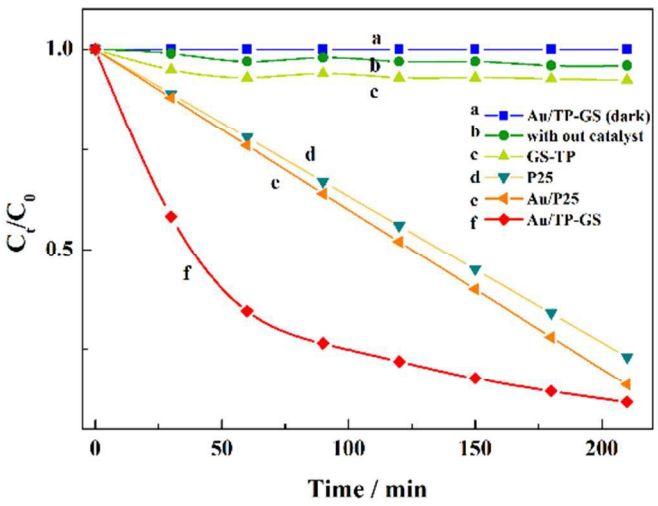

Fig. 8 Degradation of RhB (a) on Au/TP-GS in the Dark, and (b) Without catalyst, over (c) TP-GS, (d) P25, (e) Au/P25 and (f) Au/TP-GS Under Visible Light Irradiation.

The results of the photodegradation of RhB by using various catalysts such as Au/TP-GS, TP-GS, P25 and Au/P25 are shown in Fig. 8. As can be seen the RhB was very stable under visible light irradiation without a catalyst or on the Au/TP-GS in the dark. It was slightly degraded in the presence of TP-GS. However, in the presence of Au/TP-GS, the RhB degradation was remarkably enhanced. The rate constant was calculated to be about 5.01×10^{-3} min^{-1}, much larger than that of P25 (3.67×10^{-3} min^{-1}), Au deposited P25 (Au/P25, 4.0×10^{-3} min^{-1}) and TP-GS (2.6×10^{-4} min^{-1}).

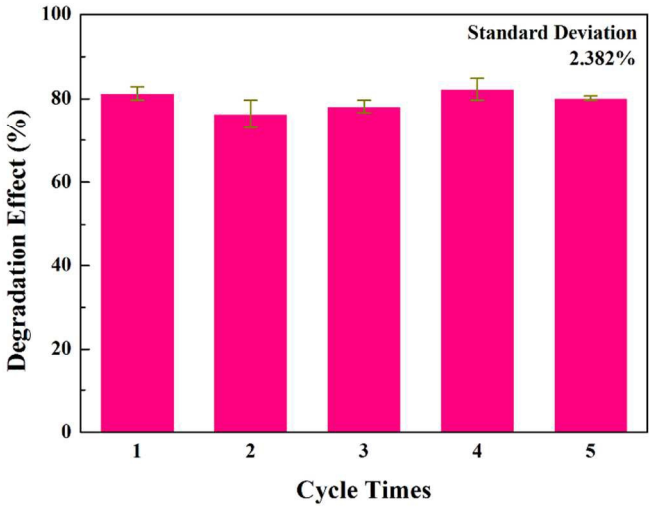

Fig. 9 Reusability experiment of Au/TP-GS as a catalyst for the photodegradation of RhB.

To evaluate the chemical stability of the catalyst, the experiments for the catalytic decomposition of dyes were performed in Fig. 9. The reused Au/TP-GS showed very little change in the catalytic activity in the case of RhB within 250 min each time. This emphasizes the excellent chemical stability of the Au/TP-GS and an indication of its long-term stability. This result is noteworthy from the viewpoint of practical application as the enhanced catalytic activity and prevention of catalyst deactivation will lead to more cost-effective operation.

The reaction mechanism that we propose is in accordance with the related reports.[10] We believe that compared to TiO_2 and its derivatives, the Au/TP-GS photocatalyst has some important attributes such as high adsorption toward organic dyes, strong π-π interaction with dye chromophores including the many desirable electrical properties of graphene.

The high activity in both the catalytic reaction of 4-NP to 4-AP and the photodegradation of RhB can be attributed to the synergistic effect of the TP-GS and Au NPs which can be explained as follows: (1) A high concentration of aromatic compounds which contain benzene rings such as 4-NP or RhB near the Au NPs on the TP-GS allows the graphene to efficiently adsorb these aromatics via π-π stacking interactions, providing excellent contact between the 4-NP and the Au NPs.[47] (2) The thiol ligand can have a role in the enhancement of the catalytic activity because it can create unique environments on the surface of Au NPs that influence activity and selectivity.[48] (3) The Au NPs of the Au/TP-GS possess a narrow size distribution, very small particle size, uniform distribution and perfect crystal structure which allows the catalyst to efficiently increase the utilization of the gold increasing the activity of the catalyst above that of larger size metal/graphene composites (such as 4.7 nm and 8-25 nm Au NPs on graphene[22, 45]) and many traditional catalysts such as Pd/C, P25 etc.

Conclusion

In conclusion, a thiophenol functionalized GS supported Au nanoparticles was successfully catalyzed using a facile synthetic approach. The method is simple, convenient and efficient. The synthesized Au/TP-GS catalyst exhibited superior catalytic activity toward both the reduction of 4-NP and the photodegradation of rhodamine B, because of the very small particle size of Au and the synergistic effect between the TP-GS and Au NPs. This method provides an easy way to effectively synthesize a low-cost Au-based catalyst for 4-NP reduction and for rhodamine B photodegradation and shows promise for the development of other useful materials.

Acknowledgement

This research was supported by the Fundamental Research Funds for the Central Universities (lzujbky-2013-234) and the Fundamental Research Funds for the Central Universities (No. 861605).

Notes

State Key Laboratory of Applied Organic Chemistry, Gansu Provincial Engineering Laboratory for Chemical Catalysis and College of Chemistry and Chemical Engineering, Lanzhou University, Lanzhou, 730000, P. R. China.
E-mail: majiantai@lzu.edu.cn; Fax: +86 931 8912577

Electronic Supplementary Information (ESI) available: [details of any supplementary information available should be included here]. See DOI: 10.1039/b000000x/

1. A. Balanta, C. Godard and C. Claver, *Chemical Society reviews*, 2011, **40**, 4973-4985.
2. A. Mohanty, N. Garg and R. Jin, *Angewandte Chemie*, 2010, **49**, 4962-4966.
3. Y.-C. Chang and D.-H. Chen, *Journal of Hazardous Materials*, 2009, **165**, 664-669.
4. K. Kuroda, T. Ishida and M. Haruta, *Journal of Molecular Catalysis A: Chemical*, 2009, **298**, 7-11.
5. M. Haruta, *Chemical record*, 2003, **3**, 75-87.
6. A. S. Hashmi and G. J. Hutchings, *Angewandte Chemie*, 2006, **45**, 7896-7936.
7. A. Abad, P. Concepcion, A. Corma and H. Garcia, *Angewandte Chemie*, 2005, **44**, 4066-4069.
8. A. Abad, C. Almela, A. Corma and H. Garcia, *Chemical communications*, 2006, 3178-3180.
9. I. M. Arabatzis, T. Stergiopoulos, D. Andreeva, S. Kitova, S. G. Neophytides and P. Falaras, *Journal of Catalysis*, 2003, **220**, 127-135.
10. Z. Xiong, L. L. Zhang, J. Ma and X. S. Zhao, *Chemical communications*, 2010, **46**, 6099-6101.
11. W. Zhu, R. Michalsky, Ö. Metin, H. Lv, S. Guo, C. J. Wright, X. Sun, A. A. Peterson and S. Sun, *Journal of the American Chemical Society*, 2013, **135**, 16833-16836.
12. Q.-Y. Bi, X.-L. Du, Y.-M. Liu, Y. Cao, H.-Y. He and K.-N. Fan, *Journal of the American Chemical Society*, 2012, **134**, 8926-8933.
13. Y. Du, H. Chen, R. Chen and N. Xu, *Applied Catalysis A: General*, 2004, **277**, 259-264.
14. S. Saha, A. Pal, S. Kundu, S. Basu and T. Pal, *Langmuir : the ACS journal of surfaces and colloids*, 2009, **26**, 2885-2893.
15. Q. Li, S. Mahendra, D. Y. Lyon, L. Brunet, M. V. Liga, D. Li and P. J. J. Alvarez, *Water Research*, 2008, **42**, 4591-4602.
16. D. Zhang, *Polish Journal of Chemical Technology*, 2012, **14**, 6.
17. J. Hu, Y.-l. Dong, Z. u. Rahman, Y.-h. Ma, C.-l. Ren and X.-g. Chen, *Chemical Engineering Journal*, 2014, **254**, 514-523.
18. F. Shi, Q. Zhang, Y. Ma, Y. He and Y. Deng, *Journal of the American Chemical Society*, 2005, **127**, 4182-4183.
19. J.-H. Chen, J.-N. Lin, Y.-M. Kang, W.-Y. Yu, C.-N. Kuo and B.-Z. Wan, *Applied Catalysis A: General*, 2005, **291**, 162-169.
20. S. Ivanova, V. Pitchon, Y. Zimmermann and C. Petit, *Applied Catalysis A: General*, 2006, **298**, 57-64.
21. Y. Guan and E. J. M. Hensen, *Applied Catalysis A: General*, 2009, **361**, 49-56.
22. S. Li, S. Guo, H. Yang, G. Gou, R. Ren, J. Li, Z. Dong, J. Jin and J. Ma, *Journal of Hazardous Materials*, 2014, **270**, 11-17.
23. Y. Zhang, S. Liu, W. Lu, L. Wang, J. Tian and X. Sun, *Catalysis Science & Technology*, 2011, **1**, 1142-1144.
24. A. K. Geim and K. S. Novoselov, *Nat Mater*, 2007, **6**, 183-191.
25. S. Guo, S. Dong and E. Wang, *ACS Nano*, 2009, **4**, 547-555.
26. S. Li, H. Yang, Z. Dong, S. Guo, J. Zhao, G. Gou, R. Ren, J. Huang, J. Jin and J. Ma, *Catalysis Science & Technology*, 2013, **3**, 2303.
27. S. Guo, S. Li, T. Hu, G. Gou, R. Ren, J. Huang, M. Xie, J. Jin and J. Ma, *Electrochimica Acta*, 2013, **109**, 276-282.
28. S. Li, Z. Dong, H. Yang, S. Guo, G. Gou, R. Ren, Z. Zhu, J. Jin and J. Ma, *Chemistry*, 2013, **19**, 2384-2391.
29. Z.-Z. Zhu, Z. Wang and H.-L. Li, *Journal of Power Sources*, 2009, **186**, 339-343.
30. A. C. Ferrari and D. M. Basko, *Nature nanotechnology*, 2013, **8**, 235-246.
31. D. Graf, F. Molitor, K. Ensslin, C. Stampfer, A. Jungen, C. Hierold and L. Wirtz, *Nano Letters*, 2007, **7**, 238-242.
32. K. N. Kudin, B. Ozbas, H. C. Schniepp, R. K. Prud'homme, I. A. Aksay and R. Car, *Nano Letters*, 2007, **8**, 36-41.
33. X. Zhong, J. Jin, S. Li, Z. Niu, W. Hu, R. Li and J. Ma, *Chemical communications*, 2010, **46**, 7340-7342.
34. D. I. Gittins and F. Caruso, *Angewandte Chemie International Edition*, 2001, **40**, 3001-3004.
35. J. Zhao, L. Zhang, T. Chen, H. Yu, L. Zhang, H. Xue and H. Hu, *The Journal of Physical Chemistry C*, 2012, **116**, 21374-21381.
36. J. Poppenberg, S. Richter, E. Darlatt, C. H. H. Traulsen, H. Min, W. E. S. Unger and C. A. Schalley, *Surface Science*, 2012, **606**, 367-377.
37. L. P. Kazansky, I. A. Selyaninov and Y. I. Kuznetsov, *Applied Surface Science*, 2012, **259**, 385-392.
38. J. Zeng, Q. Zhang, J. Chen and Y. Xia, *Nano Letters*, 2009, **10**, 30-35.
39. M. Schrinner, M. Ballauff, Y. Talmon, Y. Kauffmann, J. Thun, M. Möller and J. Breu, *Science*, 2009, **323**, 617-620.
40. E. Seo, J. Kim, Y. Hong, Y. S. Kim, D. Lee and B.-S. Kim, *The Journal of Physical Chemistry C*, 2013, **117**, 11686-11693.
41. S. Wunder, Y. Lu, M. Albrecht and M. Ballauff, *ACS Catalysis*, 2011, **1**, 908-916.
42. X. Zhou, W. Xu, G. Liu, D. Panda and P. Chen, *Journal of the American Chemical Society*, 2009, **132**, 138-146.
43. K. Esumi, K. Miyamoto and T. Yoshimura, *Journal of colloid and interface science*, 2002, **254**, 402-405.
44. K. Hayakawa, T. Yoshimura and K. Esumi, *Langmuir : the ACS journal of surfaces and colloids*, 2003, **19**, 5517-5521.
45. J. Li, C.-y. Liu and Y. Liu, *Journal of Materials Chemistry*, 2012, **22**, 8426-8430.
46. C. Chen, W. Zhao, P. Lei, J. Zhao and N. Serpone, *Chemistry*, 2004, **10**, 1956-1965.
47. Ö. Metin, S. Ho, C. Alp, H. Can, M. Mankin, M. Gültekin, M. Chi and S. Sun, *Nano Res.*, 2013, **6**, 10-18.
48. N. J. Costa and L. M. Rossi, *Nanoscale*, 2012, **4**, 5826-5834.

